Malaysian Journal of Chemistry, 2025, Vol. 27(5), 121-130
(Special Issue: *5th IKMPB Online Symposium, IKMPB 2025*)

Morphological, Structural and Photocatalytic Properties of Urea-derived Carbon-doped ZnO Synthesized via Co-precipitation for Methylene Blue Dye Degradation

Nur Liyana Izzati Aminuddin[1], Hartini Ahmad Rafaie[2]*, Zul Adlan Mohd Hir[1], Shaari Daud[1], Hamizah Mokhtar[1] and Nurul Fatahah Asyqin Zainal[2]

[1]Faculty of Applied Sciences, Universiti Teknologi MARA, UiTM Cawangan Pahang, Kampus Jengka, 26400 Bandar Tun Abdul Razak Jengka, Pahang, Malaysia

[2]Centre of Foundation Studies, Universiti Teknologi MARA, Cawangan Selangor, Kampus Dengkil, 43800 Dengkil, Selangor, Malaysia

*Corresponding author (e-mail: hartinirafaie@uitm.edu.my)

Synthetic dyes such as methylene blue (MB) pose significant environmental challenges due to their toxicity and persistence in aquatic ecosystems. In this study, pure and urea-derived carbon-doped ZnO photocatalysts were synthesized via the co-precipitation method to evaluate their efficiency in degrading MB under UV light irradiation. Urea was incorporated as a carbon source in varying weight percentages (1, 3, and 5 wt.%) to enhance the photocatalytic properties of ZnO. The morphological and structural characteristics of the prepared samples were analyzed using Scanning Electron Microscopy (SEM), Mapping-Energy Dispersive X-ray Spectroscopy (EDX), and Fourier Transform Infrared Spectroscopy (FTIR). SEM images revealed agglomerated spherical grains densely distributed across the samples, while EDX mapping confirmed the presence of carbon in the urea-doped ZnO. FTIR analysis revealed the incorporation of carbon species from urea into the ZnO lattice, resulting in lattice distortions and alteration to vibrational properties, as indicated by shifts in Zn–O peaks and the emergence of C=O vibrations, suggesting surface modifications that enhance photocatalytic performance. The photocatalytic activity of urea-derived carbon-doped ZnO demonstrated significant enhancement compared to pure ZnO, with the 5 wt.% urea-derived carbon-doped ZnO, achieving a 66.71% degradation of MB within one hour of UV exposure. These findings suggest that urea-derived carbon-doped ZnO is a promising photocatalyst for dye removal in wastewater treatment applications.

Keywords: Co-precipitation; methylene blue dye; photocatalytic; urea; ZnO

Received: April 2025; Accepted: August 2025

Water contamination caused by the widespread use of dyes in industries such as textiles, printing, cosmetics, and leather has become a significant environmental concern [1]. The aromatic and complex molecular structure of dyes renders them resistant to degradation, making them highly stable against oxidizing agents and difficult to biodegrade [2]. As a result, dye pollutants persist in the environment at high concentrations, posing serious risks to human health, aquatic ecosystems, and wildlife. Therefore, developing efficient and effective techniques to remove dye waste is crucial for maintaining ecological balance and safeguarding human health. Recent research on various wastewater treatment methods, including adsorption, biodegradation, coagulation, chemical treatments, advanced oxidation processes (AOPs), and membrane processes, have been explored. Among these, AOPs have emerged as one of the most promising approaches for organic dye degradation due to cost-effectiveness, simplicity, and ability to break down dye molecules into less harmful byproducts such as carbon dioxide (CO_2), water, and non-toxic intermediates [3, 4]. Among the numerous AOPs, photocatalysis is recognized as a viable, renewable, and environmentally friendly approach for wastewater treatment [5]. Photocatalysis uses a photocatalyst, which is typically a semiconductor material, and light for the treatment of organic compounds in wastewater. When light irradiates these materials, photo-excited charges initiate electrochemical reactions on the catalyst surface, decomposing pollutants completely or partially into harmless intermediates.

Amongst the variety of photocatalysts being investigated, zinc oxide (ZnO) is still a widely researched photocatalyst because of its remarkable physicochemical properties. ZnO possesses a direct wide bandgap of approximately 3.37 eV and a high exciton binding energy of 60 meV at room temperature, making it highly suitable for UV light-based photocatalytic activities [6,7]. Additionally, ZnO has a superior photosensitivity, high electron mobility, and environmental friendliness have established it as a compelling alternative to titanium dioxide (TiO_2) for applications in water and organic pollutant degradation. Its unique optical and electronic

†Paper presented at the 5th IKMPB Online Symposium: Sustainable Chemistry Innovations Shaping the Future Life

properties, combined with its low cost and ease of synthesis, further strengthen its appeal for large-scale applications in advanced oxidation processes (AOPs). However, despite its advantages, ZnO faces several inherent limitations that hinder its practical implementation as a standalone photocatalyst. Its wide bandgap restricts light absorption to the UV region, which constitutes only ~4% of the solar spectrum, significantly limiting its efficiency under natural sunlight [8, 9]. Furthermore, ZnO suffers from rapid recombination of photogenerated electron-hole pairs, which reduces its quantum efficiency and photocatalytic performance [6, 10]. Studies have shown that the high recombination rate not only reduces the generation of reactive oxygen species (ROS) but also limits the degradation of pollutants into less harmful byproducts. Another critical issue with ZnO is its susceptibility to photocorrosion under prolonged irradiation. During photocatalytic processes, photoinduced holes can oxidize ZnO itself, leading to a gradual loss of material integrity and performance [11]. This instability restricts its long-term use in environmental remediation applications. Additionally, the limited surface area and insufficient active sites of pure ZnO alone further constrain its photocatalytic efficiency, particularly in treating high concentrations of pollutants.

To address these limitations, several strategies have been proposed, including doping ZnO with metal or non-metal elements, forming heterojunctions with other semiconductors, and incorporating carbon-based materials [6]. Among these approaches, carbon doping has been identified as a promising method to enhance ZnO's photocatalytic activity. By introducing carbon dopants, the bandgap of ZnO can be effectively narrowed, allowing for better utilization of visible light and improved charge separation [12]. Furthermore, carbon doping can introduce mid-gap states that act as trapping sites for electrons or holes, thereby reducing recombination rates and enhancing photocatalytic efficiency. These modifications not only improve light absorption but also facilitate the separation and migration of charge carriers, which are critical for achieving high photocatalytic performance [13, 14]. Among the various carbon precursors, urea has been widely used due to its low cost, abundance, and ability to release carbon and nitrogen species during thermal treatment [15,16]. When urea is thermally decomposed, it generates carbon and nitrogen species that can be incorporated into the ZnO lattice or adsorbed onto its surface, leading to the formation of carbon-doped ZnO or ZnO-based composites. Although urea-derived carbon doping shows great potential for improving ZnO's photocatalytic properties, this area has not been studied extensively. In this study, urea as a carbon source was doped into ZnO photocatalysts using a one-step chemical co-precipitation method. This approach aims to overcome the inherent limitations of pure ZnO, such as its wide bandgap and high electron-hole recombination rate, while enhancing its photocatalytic efficiency for the degradation of methylene blue dye. The findings of this study are expected to contribute to the development of sustainable and efficient photocatalytic systems for environmental remediation, offering a viable solution for the treatment of dye-contaminated wastewater.

MATERIALS AND METHODS

Materials

The materials used in this study included zinc acetate dihydrate ($Zn(CH_3CO_2)_2 \cdot 2H_2O$, Sigma-Aldrich, ≥99% purity), urea (CH_4N_2O, Sigma-Aldrich, ≥99%), sodium hydroxide (NaOH, Merck, 98%), and methylene blue (MB, R&M Chemicals). All chemicals were used as received, without further purification. Deionized (DI) water was used throughout all experiments.

Preparation of Urea-derived Carbon-doped ZnO Photocatalyst

Urea-derived carbon-doped ZnO photocatalysts were synthesized using a co-precipitation method (Figure 1). Various weight percentages (wt.%) of urea: 0 %, 1 %, 3 %, and 5 % were employed to investigate the effect of doping level. The prepared samples were labelled as UZ-0, UZ-1, UZ-3, and UZ-5, respectively. The synthesis procedure involved dissolving zinc acetate dihydrate (0.1 mol/L) and urea (1 wt.%, 3 wt.%, and 5 wt.%) in 100 mL of DI water. For the control sample (UZ-0), urea was excluded, and the same procedure was followed. Sodium hydroxide (NaOH, 0.5 M) was added dropwise to the solution under continuous stirring until the pH of the mixture reached 10. The resulting mixture was heated and stirred at 95°C for 1 hour using a magnetic stirrer. The precipitate formed was washed several times with DI water to remove residual impurities, followed by filtration. The cleaned precipitates were dried overnight at 80°C in an oven and subsequently calcined at 500°C for 1 hour to obtain the final urea-derived carbon-doped ZnO photocatalysts.

Characterization Methods

A scanning electron microscope (TESCAN VEGA3) operating at 20 kV, equipped with an energy dispersive X-ray (EDX) analyser was used to analyse the surface morphology and composition of the samples. FTIR spectroscopy (PerkinElmer Spectrum 100) was used to identify the vibrational modes, and functional groups present in the samples within the range of 500–4000 cm^{-1}.

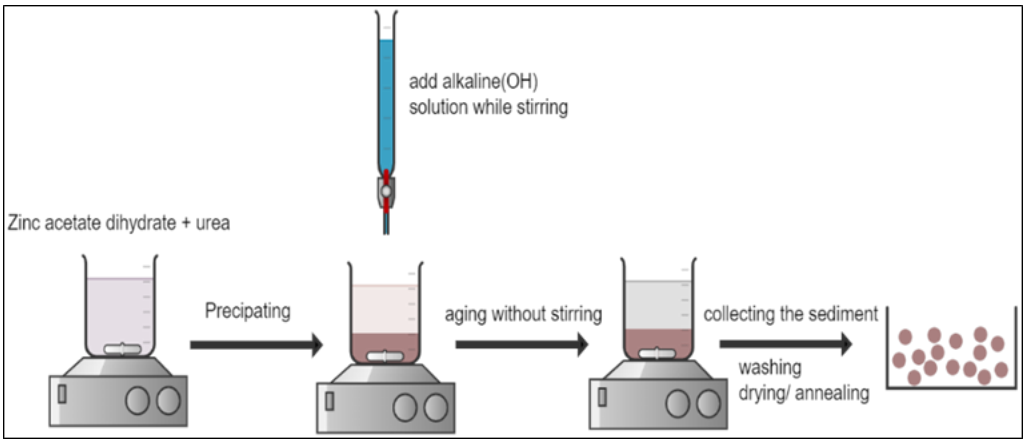

Figure 1. Schematic diagram of the co-precipitation method used in this study for preparation urea-derived carbon-doped ZnO.

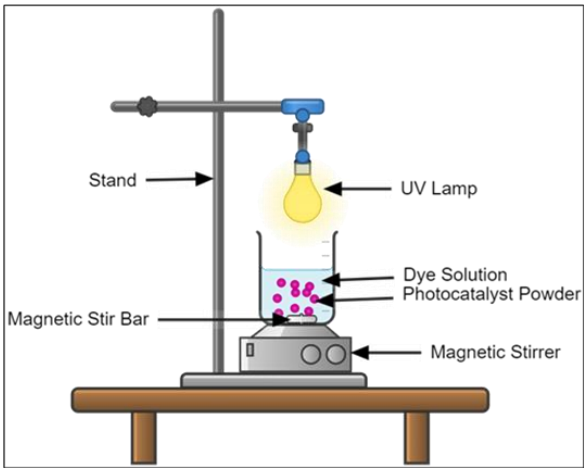

Figure 2. Schematic diagram of the photocatalytic degradation setup used in the experiments.

Photodegradation of Methylene Blue (MB) Dye under UV Light Irradiation

The photocatalytic activity of pure ZnO (UZ-0) and urea-derived carbon-doped ZnO (UZ-1, UZ-3, UZ-5) was determined by monitoring the photocatalytic degradation of methylene blue (MB) dye under UV light irradiation. A UV lamp emitting at 365 nm (12 W, 230 V, 50 Hz) was used as the irradiation source. The lamp was positioned horizontally 10 cm above the surface of the reaction mixture (Figure 2).

The measurement was conducted using a 200 mL beaker. Typically, 20 mg of the prepared photocatalyst was dispersed in a beaker containing 100 mL of a 10 mg/L MB solution. Before UV irradiation, the suspension was stirred in the dark for 30 minutes to achieve adsorption-desorption equilibrium between the photocatalyst and the MB solution. The solution was then irradiated with the UV lamp for 60 minutes, with continuous stirring. After photo irradiation, samples of 5mL were drawn at 10 minutes intervals throughout the experiment. The concentration of each sample was then analysed using a UV-Vis spectrophotometer (PerkinElmer Lambda 35) at λ_{max} = 664 nm, and the data were converted into the corresponding concentration (C) to evaluate the degradation efficiency. The degradation percentage was determined using Equation (1), respectively [17]:

$$Degradation\ percentage\ (\%) = \frac{(C_o - C_t)}{C_o}\ x\ 100 \quad (1)$$

Where C_o is the initial concentration of paracetamol and C_t is the final concentration at time t.

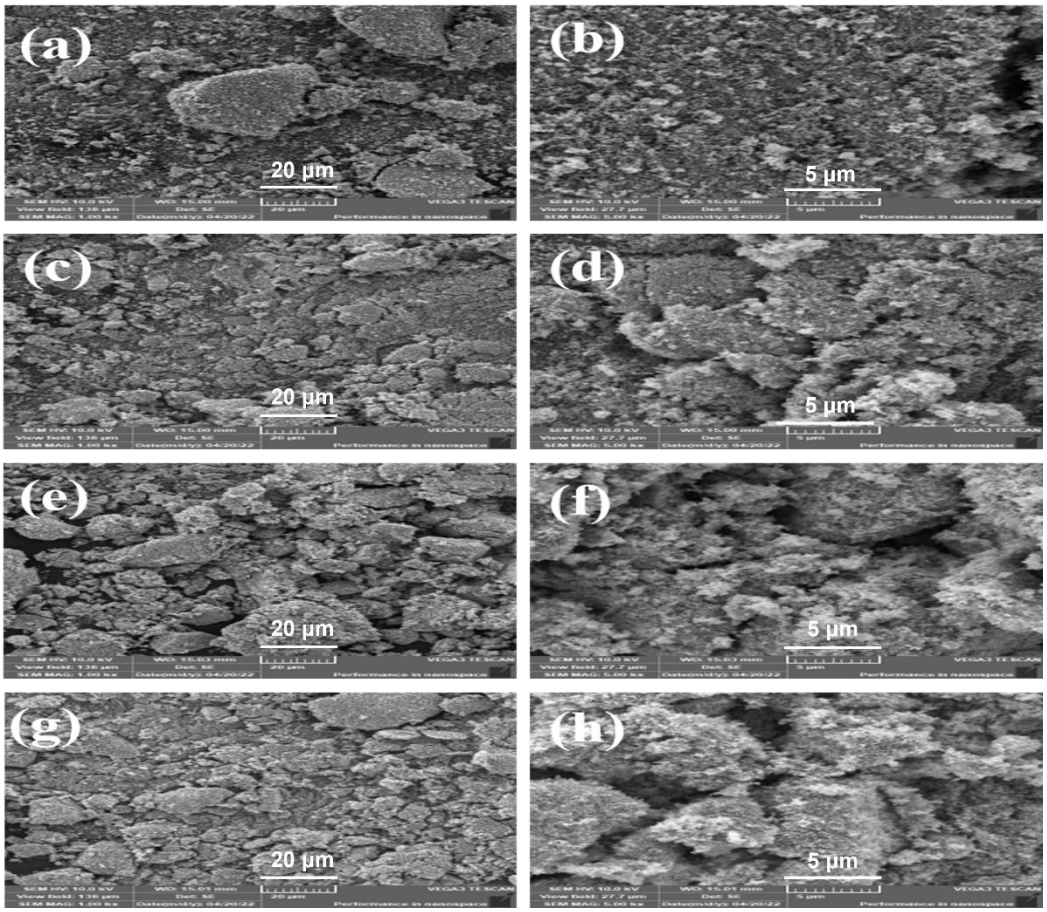

Figure 3. SEM images of (a, b) UZ-0 (c, d) UZ-1, (e, f) UZ-3, and (g, h) UZ-5 at 1,000x (left) and 5,000x (right) magnifications.

RESULTS AND DISCUSSION

Morphological structures

The morphological structures of pure ZnO (UZ-0) and urea-derived carbon-doped ZnO samples with varying weight percentages of urea (1 wt.%, 3 wt.%, and 5 wt.%), denoted as UZ-1, UZ-3, and UZ-5, were investigated using the scanning electron microscopy (SEM) technique. Figure 3 presents the SEM micrographs of the prepared samples, captured at magnifications of 1,000x (left) and 5,000x (right). The images reveal densely packed and uniformly distributed particles across all samples, with distinct morphological variations observed between the pure and urea-derived carbon-doped ZnO.

For pure ZnO (UZ-0), the particles exhibited a uniform distribution with a smooth surface morphology. In contrast, the urea-derived carbon-doped samples (UZ-1, UZ-3, and UZ-5) displayed agglomerated particles with a dense, tightly packed structure and rougher surface texture. These changes are attributed to the incorporation of carbon derived from urea during the doping process. However, increasing the urea concentration from 1 wt.% to 5 wt.% did not induce significant alterations in particle size or shape, indicating that the overall morphology remained largely consistent across samples. This observation aligns with previous reports, emphasizing that urea affects surface chemistry more than bulk morphology [18]. Additionally, the SEM images at higher magnification revealed that UZ-0 (Figure 3b) appeared more compact and with lower surface roughness compared to the urea-doped samples, suggesting surface modifications due to carbon doping (Figure 3d, 3f, and 3h). This variation in surface texture suggests that carbon doping introduced surface defects or increased the surface area, both of which are critical for enhancing photocatalytic performance. Surface defects, such as oxygen vacancies or interstitial carbon, act as trapping sites for electrons and holes, reducing recombination rates and thereby enhancing photocatalytic efficiency [16].

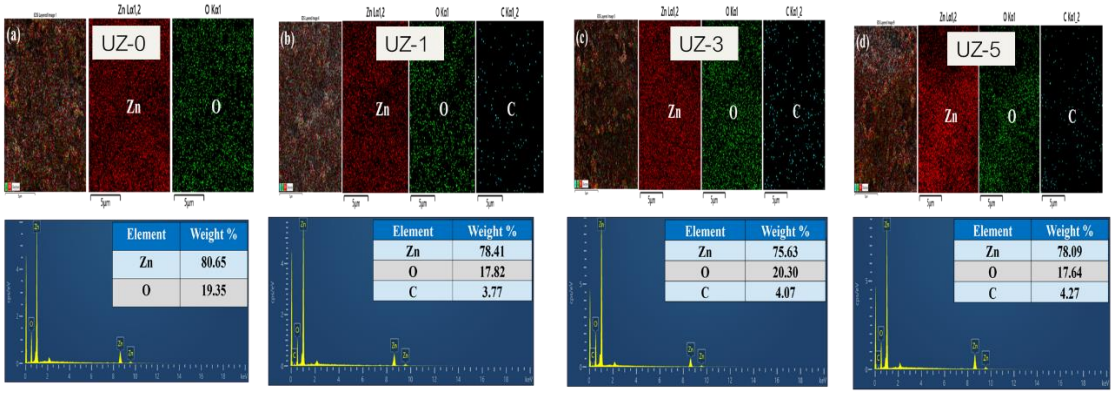

Figure 4. EDX characterization, elemental mapping, and spectrum of pure ZnO and urea-derived carbon-doped ZnO at different weight %.

EDX Mapping Analysis

The EDX mapping analysis, as depicted in Figure 4, confirms the presence of carbon (C), zinc (Zn), and oxygen (O) in the synthesized samples, with no detectable impurity peaks, thereby verifying the purity of the materials. In the mapping images, Zn, O, and C elements are represented by red, green, and blue, respectively. The elemental distribution maps indicate that Zn, O, and C are uniformly distributed throughout the ZnO structure, with carbon appearing homogeneously scattered across the framework. Quantitative analysis of the dopant concentration for urea-derived carbon-doped ZnO samples with 1, 3, and 5 wt.% urea reveals a progressive increase in the carbon content, consistent with the amount of dopant introduced during synthesis. The measured carbon weight percentages in the urea-derived carbon-doped ZnO samples are 3.77%, 4.07%, and 4.27% for UZ-1, UZ-3, and UZ-5, respectively. These results are corroborated by the EDX spectra, which display a corresponding increase in the intensity of the carbon peak with higher doping concentrations. The EDX analysis thus confirms the successful incorporation of carbon into the ZnO structure, with a homogeneous distribution of elements and a progressive increase in carbon content that aligns with the designed doping levels. This evidence further supports the successful preparation of urea-derived carbon-doped ZnO samples with tailored dopant concentrations for photocatalytic applications.

Fourier Transform Infrared (FTIR) Analysis

The FTIR analysis was performed to investigate the vibrational modes, and functional groups present in pure ZnO (UZ-0) and urea-derived carbon-doped ZnO (UZ-1, UZ-3, UZ-5) synthesized with varying urea concentrations. The FTIR spectra were recorded in the 500–4000 cm^{-1} range, as shown in Figure 5, and provide valuable insights into the structural modifications induced by carbon doping. The FTIR spectrum of pure ZnO (UZ-0) shows a strong peak at 538.79 cm^{-1}, which corresponds to Zn–O stretching vibrations, and a broad band around 3300–3400 cm^{-1}, attributed to O–H stretching vibrations from surface hydroxyl groups, as previously reported in the literature [1,18,19]. A distinct peak at 862.57 cm^{-1}, observed only in UZ-0, corresponds to ZnO lattice vibrations [20]. This peak disappears in urea-derived carbon-doped ZnO samples, suggesting structural changes due to the incorporation of carbon from urea. For urea-derived carbon-doped ZnO samples (UZ-1, UZ-3, and UZ-5), the characteristic Zn–O stretching peak shifts slightly to higher wavenumbers (540.26–542.05 cm^{-1}), indicating lattice distortion caused by carbon species derived from urea. The broad O–H band remains present in all doped samples but shifts slightly to 3385.75 cm^{-1} for UZ-1, 3420.97 cm^{-1} for UZ-3, and 3394.52 cm^{-1} for UZ-5, which might be due to interactions between hydroxyl groups and urea decomposition products, respectively [16, 21]. The bands between 1736–1739 cm^{-1} and 1372–1440 cm^{-1}, which correspond to the bending and stretching vibrations of C=O and O–H, respectively, suggest the presence of carbonyl and hydroxyl functional groups. These peaks confirm the successful incorporation of urea into the ZnO structure, respectively [22, 23, 24]. These peaks confirm the successful incorporation of urea into the ZnO structure. The presence of these groups suggests that urea decomposition modifies the ZnO surface and introduces new chemical bonds, altering its vibrational properties. Overall, the FTIR results demonstrate that urea-derived carbon induces structural and surface modifications in ZnO. These modifications, observed as peak shifts and new spectral features, indicate that carbon species from urea play a critical role in creating defects and functionalizing the ZnO lattice, potentially enhancing its catalytic and adsorption properties.

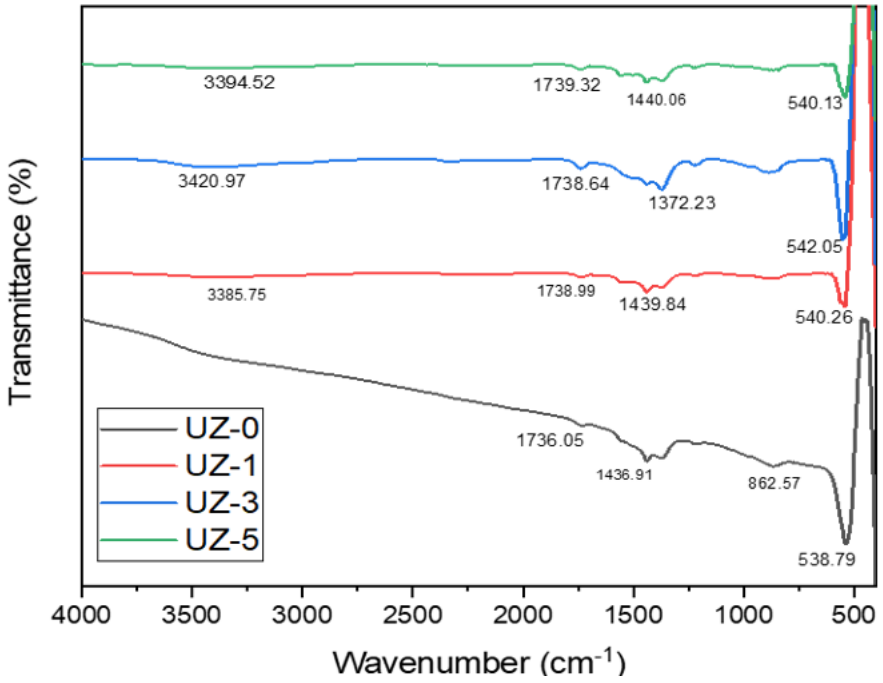

Figure 5. FTIR spectra of pure ZnO and urea-derived carbon-doped ZnO at different weight %.

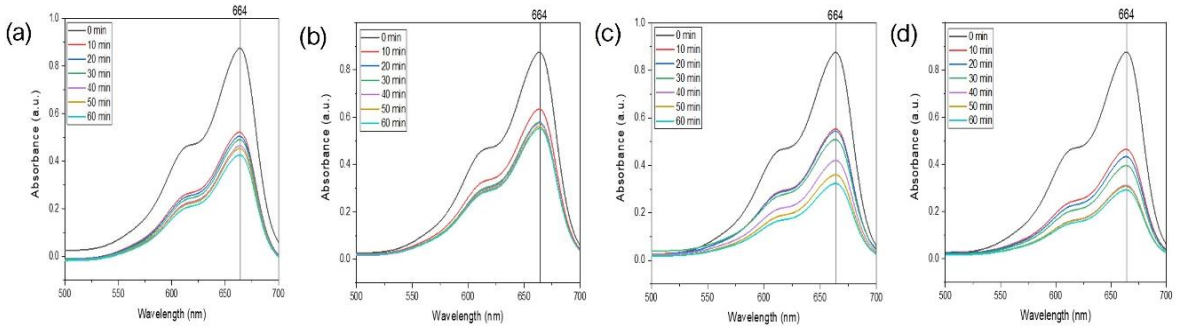

Figure 6. UV-visible absorption spectra of MB dye solution under UV lamp irradiation using (a) UZ-0, (b) UZ-1, (c) UZ-), and (d) UZ-5 as photocatalysts.

Evaluation of Photocatalytic Measurement

Photocatalytic degradation experiments were performed using methylene blue (MB) as a model pollutant, with an initial concentration of 5 mg/L. The experiments employed urea-derived carbon-doped ZnO catalysts with varying urea concentrations to evaluate their photocatalytic performance under UV irradiation for 60 minutes. Urea served as the carbon source, with doping percentages ranging from 0 to 5 wt. %. For comparison, the photocatalytic activity of pure ZnO (UZ-0) was also assessed. The results demonstrated that carbon incorporation into the ZnO lattice significantly enhanced photocatalytic activity compared to pure ZnO. As illustrated in Figure 6, the UV-visible absorption spectra of MB solutions exhibited a progressive reduction in the characteristic absorption peak at 664 nm over time, indicating the degradation of MB in the presence of the catalysts.

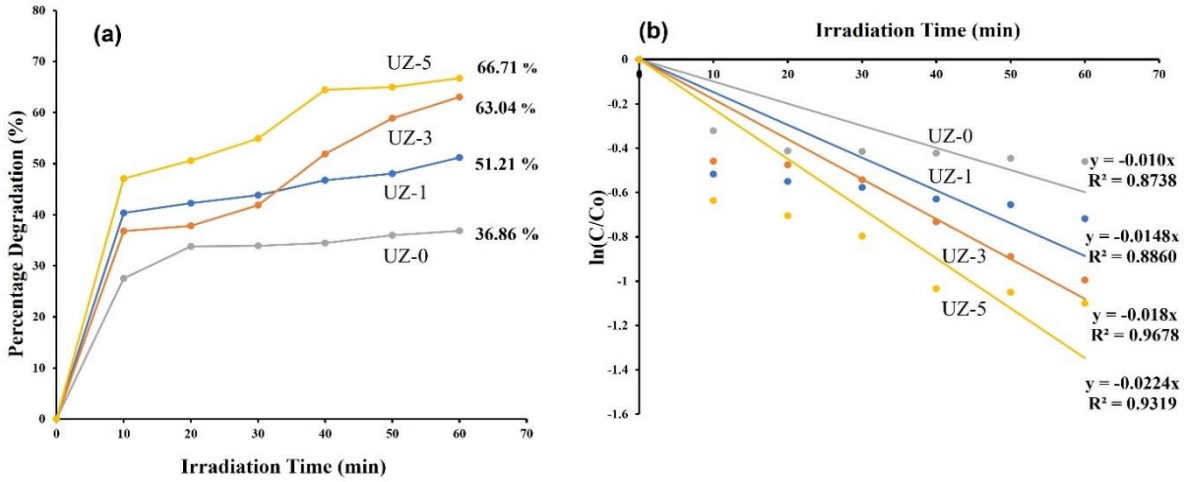

Figure 7. (a) Comparison of percentage degradation of MB dye solution under 60 min UV irradiation and (b) Plot of ln (C/Co) vs. irradiation time for the photodegradation of MB dye using pure ZnO and urea-derived carbon-doped ZnO at different weight %.

Figure 7(a) presents the photocatalytic degradation efficiencies of MB dye for all synthesized catalysts under UV irradiation, while Figure 7(b) displays the kinetic plots. The rate constant, k, was derived from the linear plot of ln(C/C₀) versus irradiation time. UZ-5 exhibited the highest rate constant of 0.0224 min^{-1}, confirming its superior degradation efficiency. The results revealed that UZ-5, containing 5 wt. % urea, achieved the highest degradation efficiency of 66.71%, compared to 36.86% for pure ZnO (UZ-0), 51.21% for UZ-1, and 63.04% for UZ-3. This enhancement in the photocatalytic performance of UZ-5 is attributed to the incorporation of carbon, which mitigates electron-hole pair recombination and facilitates the generation of reactive oxygen species (ROS) essential for organic pollutant degradation [25]. In contrast, UZ-0 exhibited the lowest degradation efficiency (36.86%), likely due to rapid electron-hole recombination, which limits the availability of ROS for dye degradation. The progressive improvement in photocatalytic activity with increasing carbon content (UZ-1 to UZ-5) suggests that carbon species act as electron traps, promoting charge separation and enhancing dye degradation efficiency [26].

To elucidate the reaction kinetics, the experimental data were analyzed using the pseudo-first-order kinetic model [17]:

$$\ln \frac{C_t}{C_o} = -kt \quad (2)$$

Where Co and Ct represent the initial and instantaneous concentrations of MB dye at times t = 0 and t = t, respectively. The rate constant, k, was derived from the linear plot ln(C/C_0) vs irradiation time. The rate constant for pure ZnO (UZ-0) was 0.0100 min^{-1}, while UZ-5, which exhibited the highest photocatalytic activity, had a rate constant of 0.0224 min^{-1}, suggesting that UZ-5 has superior degradation efficiency under UV irradiation. The improved photocatalytic performance of urea-derived carbon-doped ZnO, particularly UZ-5, is attributed to the presence of carbon species derived from urea. These carbon atoms act as electron traps, reducing electron-hole recombination and promoting charge separation. This process increases the number of reactive species, such as hydroxyl radicals (·OH), which are critical for degrading organic pollutants like MB dye [13]. As the urea concentration in the ZnO matrix increases (from UZ-0 to UZ-5), the photocatalytic efficiency improves, reaching an optimal level at 5 wt.% urea. At higher concentrations of urea (e.g., UZ-5), the carbon species provide a favourable surface interaction that facilitates the transfer of electrons from ZnO to carbon, enhancing the overall photocatalytic activity [16].

As displayed in Table 1, the photocatalytic degradation activities of MB dye were evaluated using pure ZnO and urea-derived carbon-doped ZnO with varying urea concentrations. UZ-5 demonstrated the highest degradation efficiency of 66.71% and rate constant, k of 0.0224 min^{-1}, confirming its enhanced photocatalytic performance. In contrast, UZ-0 exhibited the lowest degradation efficiency of 36.86%. The improvement in photocatalytic activity of UZ-5 is likely due to the optimal urea doping at 5 wt. %, which enhances the separation of photogenerated charge carriers and promotes the formation of reactive oxygen species responsible for pollutant degradation. In contrast, UZ-0, the pure ZnO sample, exhibited the lowest degradation efficiency at 36.86 %, likely due to the high recombination rate of electron-hole pairs, which reduces the efficiency of the photocatalytic reaction. To further clarify, minor fluctuations in UZ-1 and UZ-3 performance were not statistically significant and are likely due to minor experimental inconsistencies. These could be minimized through additional trials and improved filtration protocols.

Table 1. Photodegradation activities of urea-derived carbon-doped ZnO photocatalysts

Sample	Target Pollutant	Percentage Degradation (%)	Photodegradation Rate Constant, k (min^{-1})
UZ-0	MB dye	36.86	0.0100
UZ-1		51.21	0.0148
UZ-3		63.04	0.0180
UZ-5		66.71	0.0224

Photocatalytic Mechanism

The enhanced photocatalytic activity of urea-derived carbon-doped ZnO under UV irradiation is primarily attributed to improved charge carrier dynamics and surface reactivity induced by carbon incorporation. Upon UV light exposure, ZnO absorbs photons with energy equal to or greater than its bandgap (~3.37 eV), promoting electrons (e^-) from the valence band (VB) to the conduction band (CB), while leaving behind holes (h^+) in the VB:

$$ZnO + h\nu \rightarrow e^- (CB) + h^+ (VB) \quad (3)$$

In pure ZnO, rapid recombination of e^-–h^+ pairs limits photocatalytic efficiency. However, carbon doping introduces mid-gap states and surface defects that serve as charge-trapping sites, effectively suppressing recombination and prolonging carrier lifetimes. The photogenerated electrons react with dissolved O_2 to produce superoxide radicals ($\bullet O_2^-$):

$$e^- + O_2 \rightarrow \bullet O_2^- \quad (4)$$

Meanwhile, the photogenerated holes oxidize water or surface hydroxide ions to form hydroxyl radicals (•OH):

$$h^+ + H_2O \rightarrow \bullet OH \quad (5)$$

$$h^+ + OH^- \rightarrow \bullet OH \quad (6)$$

These reactive oxygen species (ROS) $\bullet O_2^-$ and •OH are responsible for the oxidative degradation of methylene blue (MB) into non-toxic end products [25, 26]. The presence of carbon not only facilitates charge separation but also enhances MB adsorption through increased surface defects and functional groups, thereby promoting more efficient dye degradation. The progressively higher degradation efficiency observed with increasing urea content (up to 5 wt.%) confirms the beneficial role of carbon doping in optimizing charge dynamics and catalytic performance.

CONCLUSION

In summary, urea-derived carbon-doped ZnO photocatalysts were successfully synthesized using the co-precipitation method, with varying urea weight percentages to evaluate their photocatalytic performance. Comprehensive structural and elemental characterization using SEM and EDX-mapping confirmed the uniform distribution and dense morphology of the urea-doped ZnO particles, with carbon successfully incorporated into the ZnO matrix, as evidenced by the EDX spectra. The FTIR results confirmed the presence of carbonyl and hydroxyl functional groups introduced by urea. The photocatalytic performance was evaluated through the degradation of methylene blue (MB) dye under UV irradiation. Among all samples, UZ-5 demonstrated the highest photocatalytic performance, achieving 66.71% MB degradation with a rate constant, k, of 0.0224 min^{-1}. These findings demonstrate the effectiveness of urea-derived carbon doping in enhancing photocatalytic activity. These results highlight the potential of urea-derived carbon-doped ZnO as an effective photocatalyst for dye wastewater treatment, offering a promising strategy for mitigating environmental pollution. Future studies could focus on optimizing the synthesis parameters, evaluating the degradation of a broader range of pollutants, and investigating the long-term stability and recyclability of urea-derived carbon-doped ZnO. This work provides valuable insights into the development of more efficient photocatalytic materials for large-scale wastewater treatment, particularly for industries dealing with dye effluents, contributing to sustainable environmental practices.

ACKNOWLEDGEMENT

The authors would like to express their gratitude to Universiti Teknologi MARA (UiTM) for the financial support provided through the Ministry of Higher Education, Malaysia, under the Fundamental Research Grant Scheme (FRGS) (Project Number: FRGS/1/2024/STG05/UITM/02/12). We also acknowledge UiTM Pahang Branch for offering the necessary facilities, management, and technical support to carry out this research.

The authors declare that they have no conflict of interest.

REFERENCE

1. Shubha, J. P., Kavalli, K., Adil, S. F., Assal, M. E., Hatshan, M. R. and Dubasi N. (2022)

Facile green synthesis of semiconductive ZnO nanoparticles for photocatalytic degradation of dyes from the textile industry: A kinetic approach. *Journal of King Saud University - Science*, **34**, 102047.

2. Qomariyah, L. , Kadir, A., Hirano, T., Tejamaya, M., Fauziyah, M., Putra, R. R., Sunarno, S. D. A. M. and Atmajaya, H. (2024) Sustainable removal of pigment dye from traditional batik textile wastewater using ZnO photocatalysis. *South African Journal of Chemical Engineering*, **50**, 223–234.

3. Vargas, M. A., Rivera-Muñoz, E. M., Diosa, J. E., Mosquera, E. E. and. Rodríguez-Páez, J. E (2021) Nanoparticles of ZnO and Mg-doped ZnO: Synthesis, characterization and efficient removal of methyl orange (MO) from aqueous solution. *Ceramic International*, **47**, 15668–15681.

4. Boon, C., Yong, L. and Wahab, A. (2018) A review of ZnO nanoparticles as solar photocatalysts : Synthesis, mechanisms and applications. *Renewable and Sustainable Energy Reviews*, **81**, 536–551.

5. Bhapkar, A. R. and Bhame, S. (2024) A review on ZnO and its modifications for photocatalytic degradation of prominent textile effluents: Synthesis, mechanisms, and future directions. *Journal of Environmental Chemical Engineering*, **12**, 112553.

6. Rasheed, H. M., Aroosh, K., Meng, D., Ruan, X., Akhter, M. and Cui, X. (2025) A review on modified ZnO to address environmental challenges through photocatalysis: Photo-degradation of organic pollutants. *Materials Today Energy*, **48**, 101774.

7. Abou Zeid, S. and Leprince-Wang, Y. (2024) Advancements in ZnO-Based Photocatalysts for Water Treatment: A Comprehensive Review. *Crystals*, **14**, 7.

8. Jiang, Z., Cheng, B., Zhang, L., Zhang, Z. and Bie, C. (2023) A review on ZnO-based S-scheme heterojunction photocatalysts. *Science Press*, **52**, 32–49.

9. Lim, N. Y. Y., Chiam, S. L., Leo, C. P. and Chang, C. K. (2024) Recent modification, mechanisms, and performance of zinc oxide-based photo-catalysts for sustainable dye degradation. *Hybrid Advanced*, **7**, 100318.

10. Sinar Mashuri, S. I., Kasim, M. F, Kaus, N. H. M., Tan, Y. H., Islam, A., Rashid, U., Asikin-Mijan, N, Andas, J., Taufiq-Yap, Y. H., Yaakob, M. K., Ismail, W. I. N. W. and Ibrahim, M. L. (2023) Photo-response range extension of Z-scheme ZnO/CdS for LED-light-driven photo-active catalyst. *Renewable and Sustainable Energy Reviews*,**184***,* 113602.

11. Sánchez-Cid, P., Jaramillo-Páez, C., Navío, J. A., Martín-Gómez, A. N. and. Hidalgo, M. C. (2018) Coupling of Ag2CO3 to an optimized ZnO photocatalyst: Advantages vs. disadvantages. *Journal of Photochemistry and Photobiology A: Chemistry*, **369**, 119–132.

12. Hosny, N. M. , Gomaa, I., Elmahgary, M. G. and Ibrahim, M. A. (2023) ZnO doped C: Facile synthesis, characterization and photocatalytic degradation of dyes. *Scientific Reports*, **13**, 1–12.

13. Zhang, X., Qin, J., Hao, R., Wang, L., Shen, X., Yu, R., Limpanart, S., Ma, M. and Liu, R. (2015) Carbon-Doped ZnO Nanostructures: Facile Synthesis and Visible Light Photocatalytic Applications. *The Journal of Physical Chemistry C*, **119**, 20544–20554.

14. Joy, A., Viswanathan, M. R., Vijayan, B. K., Silva, C. G., Basheer, I., Sugathan, S., Mohamed, P. A., Solaiappan, A. and Shereef, A. (2024) Solar photocatalysts: non- metal (C, N, and S)-doped ZnO synthesized through an industrially sustainable in situ approach for environmental remediation applications. *RSC Advanced*, **14**, 21655–21667.

15. Liu, X., Chen, J., Li, J., Zhong, J. and Wang, T. (2018) Enhanced sunlight-driven photocatalytic performance of ZnO prepared with the assistance of urea. *Desalination Water Treatment*, **132**, 226–234.

16. Uysal, B., Şen, S. and Top, A. (2020) Photo-catalytic and optical properties of zinc oxide structures prepared at different urea concentrations. *Revista Romana de Materiale/ Romanian Journal of Materials*, **50**, 463–470.

17. Hir, Z. A. M., Mokhtar, H., Rafaie, H. A., Daud, S., Shohaimi, N. A. M. and Alam, N. M. F. H. N. (2024) Efficient photodegradation of paracetamol by TiO2/ZnO photocatalyst and prediction via Fuzzy Inference System. *Iranian Journal of Catalysis*, **14**, 1–12.

18. Thambidurai, R., Gobi, G., Chandrasekar, M., Uthrakumar, R., Inmozhi, C. and Kaviyarasu, K. (2023) ZnO nanocomposites containing Cd are synthesized with high photodegradation potential for wastewater treatment. *Journal of King Saud University - Science*, **35**, 102915.

19. Rosman, N., Salleha, W. N. W., Ismail, A. F., Jaafara, J., Harun, Z., Aziz, F., Mohamed, M. A., Ohtanie, B. and Takashima, M. (2018) Photo-catalytic degradation of phenol over visible light active ZnO/Ag2CO3/Ag2O nanocomposites

heterojunction. *Journal of Photochemistry and Photobiology A: Chemistry*, **364**, 602–612.

20. Hitkari, G., Singh, S. and Pandey, G. (2017) Nano-Structures & Nano-Objects Structural, optical and photocatalytic study of ZnO and ZnO – ZnS synthesized by chemical method. *Nano-Structures & Nano-Objects*, **12**, 1–9.

21. Wongso, V., Chen, C. J., Razzaq, A., Kamal, N. A. and Sambudi, N. S. (2019) Hybrid kaolin/ TiO2 composite: Effect of urea addition towards an efficient photocatalyst for dye abatement under visible light irradiation. *Applied Clay Science*, **180**, 105158.

22. Víctor-Román, S. (2020) Controlling the surface chemistry of graphene oxide: Key towards efficient ZnO-GO photocatalysts. *Catalysis Today*, **357**, 350–360.

23. Tian, J. Zhen, L., Debin, Z., Changlin, Y., Xingqiang, L. and Kai. Y (2018) The preparation and characterization of CaMg(CO3)2@Ag2CO3/ Ag2S/NCQD nanocomposites and their photo-catalytic performance in phenol degradation. *Journal of Nanoparticle Research*, **20(7)**.

24 Kumar, S., Kaushik, R. D. and Purohit, L. P. (2023) RGO supported ZnO/SnO2 Z-scheme heterojunctions with enriched ROS production towards enhanced photocatalytic mineralization of phenolic compounds and antibiotics at low temperature. *Journal of Colloidal Interface Science*, **632**, 196–215.

25. Kumari, V., Mittal, A., Jindal, J., Yadav, S. and Kumar, N. (2019) S-, N- and C-doped ZnO as semiconductor photocatalysts: A review. *Frontiers of Materials Science*, **13(1)**.

26. Lebedev, A., Weerasinghe, P. V. T., Anariba, F., Hwee Leng, X., Li, D. S. and Wu, P. (2022) Urea-assisted synthesis of carbon-doped BiNbO4 with oxygen vacancies and visible light photo-catalytic applications. *Materials Advanced*, **3**, 7072–7079.